Constitutive Equations for Human Saphenous Vein Coronary Artery Bypass Graft

Hynek Chlup, Lukas Horny, Rudolf Zitny, Svatava Konvickova, and Tomas Adamek

Abstract—Coronary artery bypass grafts (CABG) are widely studied with respect to hemodynamic conditions which play important role in presence of a restenosis. However, papers which concern with constitutive modeling of CABG are lacking in the literature. The purpose of this study is to find a constitutive model for CABG tissue. A sample of the CABG obtained within an autopsy underwent an inflation–extension test. Displacements were recoredered by CCD cameras and subsequently evaluated by digital image correlation. Pressure – radius and axial force – elongation data were used to fit material model. The tissue was modeled as one-layered composite reinforced by two families of helical fibers. The material is assumed to be locally orthotropic, nonlinear, incompressible and hyperelastic. Material parameters are estimated for two strain energy functions (SEF). The first is classical exponential. The second SEF is logarithmic which allows interpretation by means of limiting (finite) strain extensibility. Presented material parameters are estimated by optimization based on radial and axial equilibrium equation in a thick-walled tube. Both material models fit experimental data successfully. The exponential model fits significantly better relationship between axial force and axial strain than logarithmic one.

Keywords—Constitutive model, coronary artery bypass graft, digital image correlation, fiber reinforced composite, inflation test, saphenous vein.

I. INTRODUCTION

BIOMECHANICAL literature which deals with vein grafts is usually focused on hemodynamical problems which are believed to play the most important role in coronary artery bypass graft (CABG) failure, e.g. [1]–[3]. Large attention is also paid to a technique of an anastomosis (e.g. angle of connection), see recent paper [4] and references herein. However, papers which present relevant experimental data and constitutive models with evaluated material parameters for CABG tissue in the context of nonlinear mechanics are lacking in the literature. Hence, main goal of our study is to present constitutive models for CABG tissue based on experimental data. Experimental methods, an inflation test and data post processing, are described first. A choice of suitable material models for anisotropic nonlinear behavior follows. Finally, predictions of material models are compared.

II. EXPERIMENT

The sample of CABG tissue was harvested within autopsy at the Institute of Forensic Medicine of the Faculty Hospital Kralovske Vinohrady in Prague. The sample was obtained from 66–year–old male donor who did not die in the link with cardiovascular diseases. After autopsy the sample was stored in the saline solution for 45 hours at temperature approximately 4°C. The inflation–extension test was finished 65 hours after death. All measurements were performed under room temperature. Afterwards the specimen was moved back to the Institute of Forensic Medicine to ethic removal. For the present study, use of autopsy material from human subjects was approved by the Ethics Committee of the Faculty Hospital Kralovske Vinohrady (Prague, Czech Republic). Experiments were performed 35 months after bypass surgery.

Under reference configuration the sample had approximately tubular shape with following dimensions: outer radius R_o = 2.053mm; inner radius R_i = 1.804mm; thickness H = 0.249mm. Sizes were determined by an image analysis of photography. The length was not measured directly, it was determined within data post processing by digital image correlation. Residual strains were immeasurable by our standard equipment due to high compliance and small sizes of the specimen. The sample was dusted over by pepper and coffee powder to create an artificial surface layer with stochastic pattern. The sample was mounted into the experimental set up for the inflation–extension test. The experimental configuration was vertical and the tube had closed bottom.

The tube was pressurized manually by a syringe. After several pre–cycles (approximately 2 minutes pressurization) measurement cycles were performed. Internal pressure was measured by a pressure probe (KTS 438, Cressto, Czech Rep.) and recorded into PC by in-house software developed

H. Chlup is with the Department of Mechanics, Biomechanics and Mechatronics Faculty of Mechanical Engineering Czech Technical University in Prague, Prague, 166 07 CZE (e-mail: Hynek.Chlup@ fs.cvut.cz).

L. Horny is with Department of Mechanics, Biomechanics and Mechatronics Faculty of Mechanical Engineering Czech Technical University in Prague, Prague, 166 07 CZE. (corresponding author to provide phone: 00420-224352690; fax: 00420-233322482; e-mail: Lukas.Horny@ fs.cvut.cz).

R. Zitny is with the Department of Process Engineering Faculty of Mechanical Engineering Czech Technical University in Prague, Prague, 166 07 CZE (e-mail: Rudolf.Zitny@ fs.cvut.cz).

S. Konvickova is with the Faculty of Mechanical Engineering Czech Technical University in Prague, Prague, 166 07 CZE (e-mail: Svatava.Konvickova@ fs.cvut.cz).

T. Adamek is with the Department of Forensic Medicine of Third Faculty of Medicine Charles University in Prague and Faculty Hospital Kralovske Vinohrady, Srobarova 50, Prague, 100 34 CZE (e-mail: adamek@ fnkv.cz).

in LabView (National Instruments, USA). Kinematics of the inflation and extension was recorded by digital cameras using digital image correlation (DIC) system Q–450 (DANTEC Dynamics, Germany).

Digital image correlation is a full-field image analysis method, based on grey value digital images that can determine the contour and the displacements of an object under load in three dimensions. Using a stereoscopic sensor setup each object point is focused on a specific pixel in the image plane of the respective sensor. Knowing the imaging parameter for each sensor (intrinsic parameter) and the orientation of the sensors with respect to each other (extrinsic parameter), the position of each object point in three dimensions can be calculated.
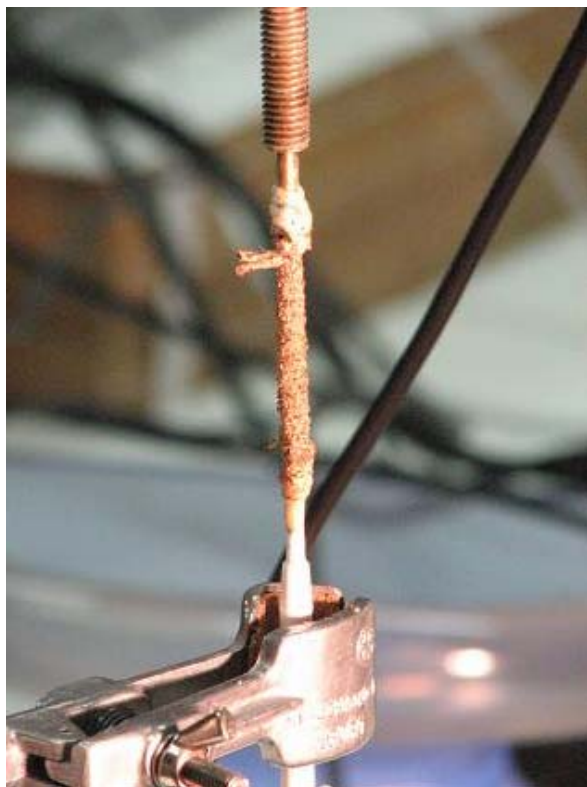

Fig. 1 The sample with dusted stochastic pattern on the surface

External loads had the form of the internal pressure and axial force. The force is originated by the pressure which is applied to the bottom of the tube (closed tube configuration). Four measurement cycles were digitally recorded. The pressure rage within the measurement was from 0 up to 20kPa. Four recorded cycles span to 60 seconds, hence the loading can be considered as quasi–static. Experimental measurements with extra weights were also performed but they are not included in present analysis. Moreover, it is not quite clear how much are bypass grafts axially pre–strained in situ.

III. DATA POSTPROCESSING

Digital image correlation system Q–450 includes data postprocessisng unit Istra (Istra 4D v. 4.2.1, DANTEC Dynamics, Germany) which enables evaluation of kinematical quantities. The principles for displacements and strain evaluation by digital image correlation are presented in [5]. Although DIC enables to evaluate local strain distributions we were focused on mean values of radial displacements and axial stretches. Their values characterize spatial configurations of measured object. It should be noted that within a regression analysis of material models the CABG was modeled as a thick walled–tube. To our knowledge, the use of DIC is not so usual as experimental method in blood vessel mechanics. But its successful application has already been reported in [6]. Recorded pressure data and evaluated displacements were arranged to match the same phase. The shift was computed by means of comparison of 12 significant points on the records. These points were regarded as temporarily coincident. Inertial and inelastic effects were neglected.

Fig. 2 The experimental setup

IV. CONSTITUTIVE MODELING AND REGRESSION

A computational model for CABG tissue under inflation and extension was based on the thick walled–tube. Performed analysis incorporates large strains. Residual and shear strains were not included. The material was supposed to be hyperelastic and incompressible. Unfortunately, we did not perform histological analysis. The graft was modeled as a one–layered tube. A presence of collagenous fibers is expected, thus the material is modeled as fiber reinforced composite. Supposed structure contains two families of collagenous fibers which are oriented helically and

symmetrically disposed. Both of them have the same mechanical response. Thus the anisotropy of the wall could be regarded as local orthotropy. This is the same structure as in paper [7]. Detailed information about local orthtropy can be found in [14].

Mechanical response of the hyperelastic material is described by a strain energy density function (SEF) and its derivatives. In the present study we performed the regression analysis for two different models. The first one is the exponential model of the SEF proposed in [7] by Holzapfel, Gasser and Ogden. This model was incorporated in the following form

$$\psi = c\left(I_1 - 3\right) + \frac{k_1}{k_2}\left(\mathbf{e}^{k_2(I_4-1)^2} - 1\right). \qquad (1)$$

Symbols in (1) have the following meaning: ψ – strain energy density function; c and k_1 – stress-like material parameters; k_2 – non-dimensional material parameter; I_1 – first invariant of right Cauchy–Green strain tensor; I_4 – fourth (pseudo)invariant of right Cauchy–Green strain tensor related to local orthotropy of the material. I_4 can be expressed in the form

$$I_4 = \lambda_t^2 \cos^2 \beta + \lambda_z^2 \sin^2 \beta . \qquad (2)$$

Here λ_t, λ_z denote stretches in the circumferential and axial directions, respectively, in the thick walled–tube. Symbol β denotes helix angle of fiber helices measured to circumferential axes. I_4 is symmetric with respect to $\pm\beta$. The form of (1) is additive split into isotropic part (Neo–Hook) related to energy stored in a matrix of composite, and exponential part related to energy stored in fibers. The model (1) was successfully used by many authors; see e.g. papers [4], [7]–[9].
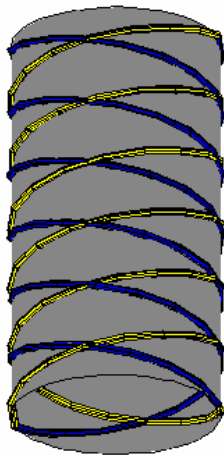

Fig. 3 The tube reinforced with two families of fibers

The second considered model of SEF is based on the concept of limiting fiber extensibility recently published by Horgan and Saccomandi [10], [11]. This is derived from a model proposed by Gent for macromolecular materials, [12]. The leading idea is that there exists a limiting value of a fiber stretch and toward this the stored energy increases unlimitedly. We consider this model in the form as follows

$$\psi = c\left(I_1 - 3\right) - \mu J_m \ \mathbf{ln}\left(1 - \frac{\left(I_4 - 1\right)^2}{J_m^2}\right). \qquad (3)$$

The meaning of symbols c and I_4 in (3) is the same as in (1) and (2). A shear modulus (stress–like parameter) is denoted μ. J_m is non-dimensional material parameter and is related to the limiting value of the stretch due to its incidence in the denominator. The limiting value of the fiber stretch is implicated by a requirement of positivity for the argument of the logarithm. Admissible fields of stretches must satisfy

$$\left(I_4 - 1\right)^2 < J_m^2 . \qquad (4)$$

It should be noted that both models of SEF represent the locally orthotropic material. It is assumed that the matrix and fibers undergo the same deformation at each point of continuum. Another successful fitting of experimental data with the model (3) for human aorta can be found in [13].

Regression analysis based on least square method gave the estimations for material parameters in the models (1) and (3). A system of nonlinear equations was solved by Levenberg – Marquardt algorithm using in-house software package FEMINA. Least square optimization was based on a comparison of measured and predicted values of the internal pressure and axial force during inflation and extension of the cylindrical tube. Computational model of the thick–walled tube predicts the internal pressure p and the axial force F in the following forms

$$p = \int_{r_i}^{r_o} \lambda_t \frac{\partial \psi}{\partial \lambda_t} \frac{dr}{r} , \qquad (5)$$

$$F = \pi \int_{r_i}^{r_o}\left(2\lambda_z \frac{\partial \psi}{\partial \lambda_z} - \lambda_t \frac{\partial \psi}{\partial \lambda_t}\right)r\,dr . \qquad (6)$$

New symbols used in (5) and (6) are r_i what denotes internal radius in the spatial configuration, and r_o what denotes outer radius in the spatial configuration. The variable radius through the wall thickness in spatial configuration is denoted r. Add that zero external pressure is supposed. Final term for least square optimization has the form of (7).

$$WSSQ = \sum_i w_i \left(p_i^{EXP} - p_i^{MOD}\right)^2 + \sum_j w_j \left(F_i^{EXP} - F_i^{MOD}\right)^2 \qquad (7)$$

In (7) $WSSQ$ means weighted sum of squares, p_i^{MOD} denotes internal pressure predicted by (5), and p_i^{EXP} means measured value of the internal pressure, respectively. Similarly F^{MOD} is the value of axial force predicted by (6), and F^{EXP} is the value of the loading force. Weights are denoted w_i and w_j. Indices denote the number of the observation point.

V. RESULTS AND CONCLUSION

The results of regression analysis are presented in the Fig. 4 and Fig. 5. Both models fit experimental data successfully. The model (1) fits better than (3), especially in the case of axial force.
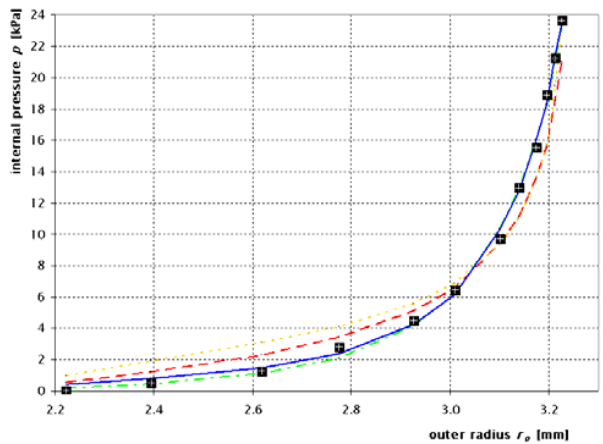

Fig. 4 Regression results: pressure–radius data and model predictions. Observation points are represented by bold boxes. Model predictions are represented by curves: (1) without Neo–Hook is represented by dash–dot curve; (1) with Neo–Hook is represented by solid curve; (3) without Neo–Hook is represented by long–dash curve; (3) with Neo– Hook is represented by dot curve.
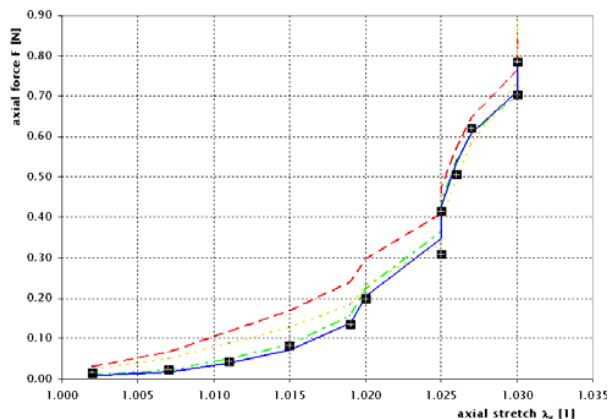

Fig. 5 Regression results: axial force–axial stretch data and model predictions. Observation points are represented by bold boxes. Model predictions are represented by curves: (1) without Neo–Hook is represented by dash–dot curve; (1) with Neo–Hook is represented by solid curve; (3) without Neo–Hook is represented by long–dash curve; (3) with Neo– Hook is represented by dot curve.

TABLE I
MATERIAL PARAMETERS

Model	c [kPa]	k_l [kPa]	k_2 [kPa]	β [°]
(1)	0	24.46	9.912	58.46
(1)	3.149	20.01	11.13	58.82
Model	c [kPa]	μ [kPa]	J_m [1]	β [°]
(3)	0	33.84	0.6919	55.24
(3)	7.625	25.38	0.6755	55.23

In order to fit material models we selected observation points from one loading cycle. Estimated material parameters are presented in the Table I. Both models were fitted twice, once with and again without Neo–Hookean member. It is established by the choice of parameter $c = 0$.

The fact that material parameters fitting is based on one cycle may cause restrictions on a domain of identified SEF models. It should be also noted that in the case of anisotropic materials the inflation test may not be sufficient to determine material parameters which are valid for different type of loadings. The material parameters presented in the Table I make strain energy function (1) and (3) convex. Despite both models have different forms predicted values of coiling angles for helical fibers are very similar. Finally, although (1) fits experimental data better than (3), the idea of limiting fiber extensibility for biological tissue seems to be very attractive to explain large strain stiffening.

REFERENCES

[1] R. L. Leask, J. Butany, K. W. Johnston, C. R. Ethier, M. Ojha, "Human saphenous vein coronary artery bypass graft morphology, geometry and hemodynamics," *Ann. Biomed. Eng.*, vol. 33, no. 3, pp. 301–309, March 2005.
[2] R. Tran–Son–Tay, *et al.*, "An experiment-based model of vein graft remodeling induced by shear stress," *Ann. Biomed. Eng.*, vol. 36, no. 7, pp. 1083–1091, July 2008.
[3] C. M. Fernandez, et al., "Impact of shear stress on early vein graft remodeling: A biomechanical analysis," *Ann. Biomed. Eng.*, vol. 32, no. 11, pp. 1484–1493, November 2004.
[4] F. Cacho, M. Doblaré and G. A. Holzapfel, „A procedure to simulate coronary artery bypass graft surgery," *Med. Bio. Eng. Cmput.*, vol. 45, pp. 819–827, August 2007.
[5] C. Herbst, K. Splitthof, "Q–400 Basics of 3D digital image correlation," [online]. Available on http://www.dantecdynamics.com/Default.aspx?ID=855.
[6] D. Zhang, C. D. Eggleton and D. D. Arola, "Evaluationg the mechanical behavior of arterial tissue using digital image correlation," Exp. Mech., vol. 42, no. 4, pp. 409 – 416, December 2002.
[7] G. A. Holzapfel, T. C. Gasser, and R. W. Ogden, "A new constitutive framework for arterial wall mechanics and a comparative study of material models," *J. Elast.*, vol. 61, no. 1–3, pp. 1–48, July 2000.
[8] J. Stalhand, "Determination of human arterial wall parameters from clinical data," *Biomechan. Model. Mechanobiol.*, (Accepted for publication).
[9] G. A. Holzapfel, G. Sommer, C. T. Gasser and P. Regitnig, "Determination of layer–specific mechanical properties of human coronary arteries with nonatherosclerotic intimal thickening and related constitutive modeling," *Am. J. Physiol. Heart Circ. Physiol.*, vol. 289, no. 5, pp. H2048–H2058, November 2005.
[10] C. O. Horgan, and G. Saccomandi, "A description of arterial wall mechanics using limiting chain extensibility constitutive models," *Biomechan. Model. Mechanobiol.*, vol. 1, no. 4, pp. 251–266, Aprile 2003.
[11] C. O. Horgan, and G. Saccomandi, "A new constitutive theory for fiber–reinforced incompressible nonlinear elastic solids," *J. Mech. Phys. Solids*, vol. 53, no. 9, pp. 1985–2015, September 2005.
[12] A. N. Gent, "New constitutive relation for rubber," Rub. Chem. Technol., vol. 69, no. 1, pp. 59–61, Mach–April 1996.
[13] L. Horny, R. Zitny, and H. Chlup, "Strain energy function for arterial walls based on limiting fiber extensibility," Proceedings of 4th European Congress for Medical and Biomedical Engineering 2008, 23–27 Nov 2008 Antwerp, Belgium, IFBME (Accepted for publication).
[14] G. A. Holzapfel, *Nonlinear solid mechanics – A continuum approach for engineering.* Chichester: John Wiley & Sons, 2000, ch. 6.